SPACE TELESCOPE SCIENCE INSTITUTE
Operated for NASA by AURA

Instrument Science Report ACS 2004-08

Detector Quantum Efficiency and Photometric Zero Points of the ACS

G. De Marchi, M. Sirianni, R. Gilliland, R. Bohlin,
C. Pavlovsky, M. Jee, J. Mack, R. van der Marel & F. Boffi
June 11, 2004

ABSTRACT

We present the characterization of the on-orbit sensitivity of the ACS CCDs cameras. Observations of spectrophotometric standard stars have been used to improve the pre-launch sensitivity and detector quantum efficiency. The new values have been implemented in SYNPHOT which is now able to reproduce the observed count rates to within 0.5% in all broad band filters. For all narrow band filters and two broadband filters (F474W and F606W) a correction factor has been applied to the original filter transmission curve to bring the predicted count rates in agreement with observations. Finally, we calculate the photometric zero points for the WFC and HRC in all three photometric systems used by Synphot, namely VEGAmag, STmag and ABmag.

1. Introduction

The purpose of the work described here is to improve the pre-launch characterization of the sensitivity and detector quantum efficiency (DQE) of the ACS, in order to allow the HST synthetic photometry software Synphot to more reliably compute photometric data such as the zero points. Since the spectro-photometric standard stars used here are white dwarfs, the update to the photometric components of Synphot does not take into account the colour terms that could arise when objects with very different spectral types are considered. These issues are addressed elsewhere (Sirianni et al. 2004). In the future, when data from more calibration standards become available, the values of the DQE, filter response curves and photometric zero points given here will most likely need to be

revised. However, any revisions are expected to be small, at the level of few percent level or less.The data used in this work have been collected during the initial calibration phase of the ACS, lasting from 2002 April through to 2003 February. More recent data will be presented in future ISRs.

2. Observations

Two spectro-photometric standard stars have been used for this programme, namely GD71 (Bohlin et al. 1995) and GRW+705824 (Oke 1990; in the following, called for simplicity GRW70). Of these, only GD71 is a primary spectrophotometric standard (Bohlin et al. 1995). For GD71, observations were collected in 2002 May, during the SMOV phase, in all filters with both the WFC and HRC cameras. GRW70 was observed four times, in the summer and fall of 2002 and early 2003 (see Appendix), through most of the filters with both cameras. Additional observations are available with the HRC in UV broad band filters. In all cases, observations with the WFC were conducted with both channels (WFC1 and WFC2), by reading out a sub-array of 512 pixel square around the target, whereas for the HRC the detector was read out in full. The default gain values of 1 and 2, respectively, were used for the WFC and HRC observations. A full list of the observations is given in Table 4 in the Appendix. In order to remove cosmic ray hits, a pair of images was obtained for each combination of camera and filter (CR-SPLIT=2).

3. Data Reduction

The data were processed via the automated pipeline, upon retrieval from the HST archive (’on the fly re-calibration’), which took care of bias and flat fielding correction as well as correction for the geometrical distortion. The analysis was carried out on the "_drz" data products (drizzle files), but the data-quality files produced for each individual frame by the pipeline (contained in the "_flt " files) were also inspected, as explained below. The exact pixel position of the standard star in each frame was obtained with the centering algorithm provided in the IRAF version of DAOphot (center) by using the centroid option. These stars are the only object detectable in their frames. The reference flatfield files used to process these images are listed in Table 4.

We note here that the ACS pipeline procedure applies to sub-array frames bias files derived by selecting from the full-frame bias the region corresponding to the sub-array. Since no over-scan is available in sub-array frames, their actual bias level and, to a lesser extent, bias shape may differ from that of the full-frame bias file. Although sub-array bias

frames were secured in the course of these calibration observations, the pipeline software available at the time when this reduction took place did not yet allow their use. On the other hand, as we explain in the following, photometric measurements were done using aperture photometry, which is insensitive to an error in the bias level. As regards the bias shape, the available data (Sirianni et al. 2002a) suggest that the bias varies relatively smoothly over the regions of 512 x 512 square pixel covered by the WFC sub-arrays near the centre of the WFC1 and WFC2 detectors. For these reasons, we do not expect the lack of reference sub-array bias frames to have affected the accuracy of our investigation.
Aperture photometry was carried out to measure the flux of each object. For the WFC a radius of 20 pixel (1 arcsec) was selected, with a background annulus ranging from 120 through to 160 pixel (6 - 8 arcsec). For the HRC a radius was selected of 40 pixel (1 arcsec), with a background annulus from 225 through to 260 pixel (5.6 - 6.5 arcsec). Encircled energy curves, built by plotting the measured count rates within apertures of increasing radius (Sirianni et al. 2004), show that a radius of 1 arcsec does not encompass the totality of the stellar flux and, more importantly, that the fraction there enclosed depends on wavelength. Therefore, we decided to define a nominal infinite aperture at 5.5 arcsec radius and we assume that within such an aperture we measure the totality of the flux. It is, however, impractical to use such a large aperture, since in some cases the stars fall too close to the edge of the frame or to the HRC coronographic fingers to permit their use. For this reason, we have decided to measure the flux within the apertures indicated above and to apply the needed aperture correction to bring it to 5.5 arcsec (see Table 1).

Since both standard stars are rather bright (V=13.03 for GD71 and V=12.77 for GRW70), relatively short exposures were used for the broad band filters (see Table 4). As a further check that no saturation or deviation from linearity had occurred near the stellar peak, the data quality files, generated by the pipeline, were carefully analyzed. Only in one case (GD71 observed with WFC1/F435W) is the central stellar pixel marked as saturated. However, this is caused by the number of electrons exceeding the limit set by the 16 bit dynamic range of the analogue-to-digital converter rather than to the saturation of the full well. Although this fact has no effect on the neighboring pixel, this particular image has not been considered in the analysis that follows. The data quality files have also been checked for possible degradation due to cosmic ray hits or defective pixels in the immediate surrounding of the stellar peak, but these effects have been found to be negligible.

Table 1. Measured count rates (e-/sec), after correction to'infinity' based on the value of the encircled energy (EE) corresponding to the selected aperture. Note the trend of the encircled energy with wavelength.

WFC	**GD71**	**GRW70**	**EE**
F435W	154910 +/- 465	180385 +/- 1219	0.942
F475W	208276 +/- 625	244366 +/- 2640	0.947
F502N	5866 +/- 37	735 +/- 41	0.950
F550M	53265 +/- 271	69139 +/- 305	0.959
F555W	124658 +/- 104	156863 +/- 915	0.952
F606W	219685 +/- 591	280053 +/- 977	0.955
F625W	110316 +/- 1410	145118 +/- 542	0.959
F658N	4973 +/- 21	6021 +/- 37	0.955
F660N	1949 +/-4	2378 +/- 58	0.960
F775W	62236 +/- 197	85822 +/- 442	0.959
F814W	75356 +/- 23	104597 +/- 467	0.959
F850LP	22297 +/- 22	31690 +/- 186	0.948
F892N	2309 +/- 48	3252 +/- 42	0.945
HRC	**GD71**	**GRW70**	**EE**
F220W	55539 +/- 151	36881 +/- 289	0.952
F250W	49751 +/- 113	37670 +/- 281	0.952
F330W	50971 +/- 22	42540 +/- 220	0.937
F344N	4696 +/- 30	4036 +/- 54	0.944
F435W	95914 +/- 294	104809 +/- 476	0.945
F475W	126241 +/- 231	148868 +/- 784	0.944
F502N	3856 +/- 20	4848 +/- 35	0.943
F550M	35826 +/- 129	46686 +/- 350	0.951
F555W	80405 +/- 310	102612 +/- 617	0.953
F606W	136786 +/- 57	177501 +/- 690	0.951
F625W	67814 +/- 321	89454 +/- 710	0.949
F658N	2941 +/- 15	3601 +/- 36	0.940
F660N	1173 +/- 9	1439 +/- 15	0.927
F775W	32428 +/- 94	45332 +/- 256	0.928
F814W	40599 +/- 41	56859 +/- 232	0.903
F850LP	14165 +/- 67	20249 +/- 165	0.820
F892N	1430 +/- 14	2058 +/- 37	0.827

4. Data Analysis

The count rates measured for each combination of detector/filter/target are shown in Table 1. They were compared with the predictions obtained by running the synthetic photometry package Synphot with the available reference files describing the various HST components (mirror reflectivity, detector quantum efficiency, filter throughput, etc.), so that these latter could be updated. The DQE reference files used for this comparison are, however, not those derived from the ground testing but those updated on the basis of the first few months of on orbit operation of the ACS, as detailed in Sirianni et al. (2002b). Regardless of the adopted starting conditions, however, the final product of this analysis is intended to replace all previous reference files.

In order to reduce the statistical uncertainty associated with the measurement process, the data for the same combination of detector and filter were averaged together. Indeed, the four epochs of observation available for GRW70 (six for UV filters) show no systematic trends, thus implying that the WFC is photometrically stable. As a measure of the observational uncertainty (see Table 1) we summed in quadrature the standard deviation of the various epochs, treating observations of the same star and filter with the WFC1 and WFC2 for the same epoch as independent quantities and the error on the aperture correction from the EE curves. For GD71 only one epoch is available so for that star the uncertainty shown in Table 1 simply reflects the photometric error (Poisson statistics) combined in quadrature with the aperture correction uncertainty.
The purpose of this project was to update the photometric zero point of each observing mode (camera/detector/filter) and, in turn, the DQE and transmission curves of all the filters. It was, however, not possible to perform these updates in isolation, one filter or wavelength at a time, since most filters cover a broad wavelength range and the same wavelength range is often covered by more than one filter. Thus, it was necessary to simultaneously compare observed and predicted count rates over the whole wavelength domain of each detector and derive incremental sensitivity updates to be applied simultaneously to all modes, so that new predictions could be derived and the procedure started over until convergence. In practice, it was decided to deal initially with broad band filters alone to obtain a more realistic description of the DQE (under the assumption that the available filter transmission curves were correct), leaving updates to medium and narrow band filters to a later stage.

This iterative approach used consists of the following steps:

1. The ratio of observed to predicted count rates for any given filter is plotted as a function of the pivot wavelength of the corresponding observing mode, defined as indicated in the ACS instrument handbook (Pavlovsky et al. 2003, Section 6.2).

2. A smooth curve is fitted to these points and is re-sampled at the same wavelengths as the DQE.
3. The DQE is multiplied by the smooth curve so obtained and the result is fed to Synphot in order to calculate a new series of the expected count rates for the modes in use.
4. The procedure resumes from step 1 until the ratio of observed and predicted count rate agrees with unity to within 0.5% for all filters.

Figures 1 and 2 show, for the WFC and HRC respectively, the initial values of the ratio of observed and predicted count rates for all filters. Squares refer to the GD71 data, whereas crosses correspond to the GRW70 measurements. It should be noted here that the WFC data points corresponding to GD71 appear systematically a few percent above those of GRW70. Since GRW70 is not a primary spectro-photometric standard, this discrepancy could in principle suggest that the spectrum of GRW70 that Synphot uses for predicting the count rates might be affected by systematical uncertainties. However, this would require it to be systematically ~1% brighter than the actual star, an amount that would have not gone unnoticed. Furthermore, the situation is not so clear-cut for the HRC, where no systematic trend is seen. So, instead of attempting a correction for this discrepancy we take the observed differences as an estimate of the uncertainty of our calibration. Observations of other spectro-photometric standard stars, planned for the forthcoming calibration cycles, will considerably reduce this uncertainty.

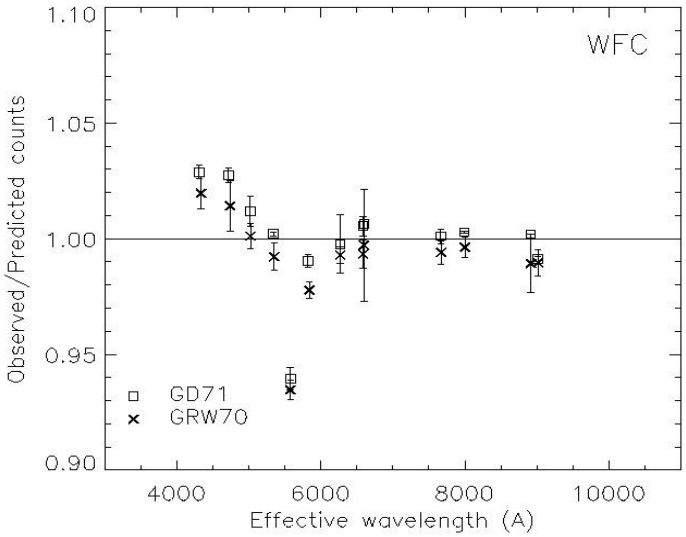

Figure 1: Initial observed/predicted count rates for the WFC. As indicated, squares correspond to GD71 whilst crosses mark the GRW70 data. Error bars are from Table 1.

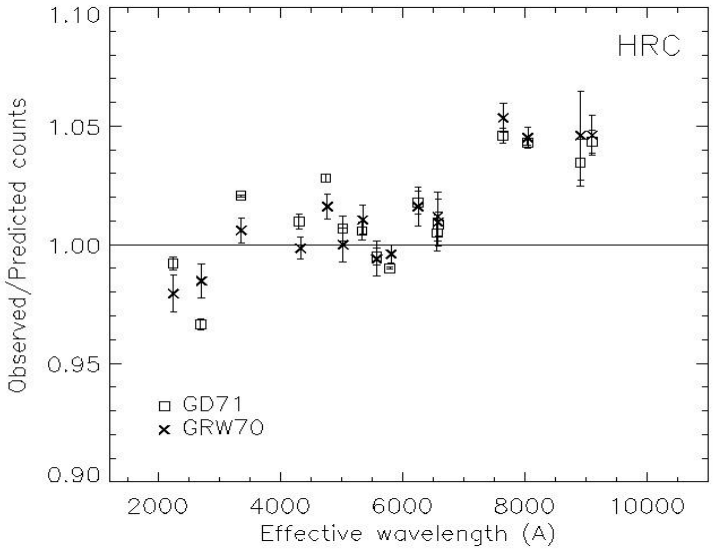

Figure 2: Initial observed/predicted count rates for the HRC. As indicated, squares correspond to GD71 whilst crosses mark the GRW70 data. Error bars are from Table 1.

5. Flat Field Uniformity And Filter Transmission Curves

Although adjacent broad band filters can considerably overlap each other, the adopted procedure should ensure rapid convergence if knowledge of the flat field and of the filter's response is accurate. An initial test of this type, conducted on the SMOV data alone (GD71) in 2002 August, revealed some discrepancies in the flat field of broad band filters, which were subsequently corrected as explained in the report by Mack et al. (2002; ACS/ISR 02-08). With the aim of further minimising the effects of flat fielding uncertainties, all observations of GRW70 were designed to have the star at the same detector location (within a few pixels). Those of GD71, although displaced by about 100 pixel in X and 100 in Y due to the initial pointing uncertainty in the early phases of SMOV, still fall in the region of the detector where the flat field is most reliable. We estimate that the corresponding uncertainty on the ACS sensitivity caused by flat field uncertainties should amount to less than 0.5% for all broad band filters.

As regards the accuracy of the available filter transmission curves, we have discovered some discrepancies which might be due to measurement uncertainties during the ground testing of the ACS. In particular, it appears that the available transmission curve of the F606W filter is not compatible with those of the F555W and F625W filters, with which it overlaps completely in wavelength. In fact, regardless of the actual shape of the DQE in the range from ~450 nm through to ~730 nm, the ratio of the observed counts and those predicted by Synphot for F606W is systematically ~ 2% smaller than the corresponding ratios for the F555W and F625W filters. This discrepancy applies to both the WFC and HRC and suggests that at least one of these three filter response curves, as measured on the ground, does not match the properties of the corresponding filter. The F555W and F625W filters, however, appear fully consistent with the other broad band filters with which they overlap, thus suggesting that the uncertainty lies in the F606W band. A similar discrepancy was found for F475W. We have, therefore, decided to exclude the F606W and F475W data from the iterative approach defined above and to correct these filters' transmission curve at a later stage, together with the medium and narrow band filters, after having established the broad properties of the DQE.

6. Results and Discussion

Figures 3 and 4 show the ratio of observed and predicted counts at the end of the iterative process, namely after 5 iterations for WFC and 7 for HRC, when discrepancies are less than 0.5% for all filters. Crosses indicate the average ratio for each filter at the end of the process, whereas the squares correspond to the same values at the beginning of it. For each filter, the squares correspond, in practice, to the average of the measurements as plotted in Figures 1 and 2. Error bars, as given in Table 1, are only shown for the final ratios but they would apply identically to the initial values as well. The final DQE curves resulting from the iterative process are shown as a dashed line in Figures 5 and 6, respectively for the WFC and HRC, where they can be directly compared with the initial values (solid lines; from Sirianni et al. 2002b).

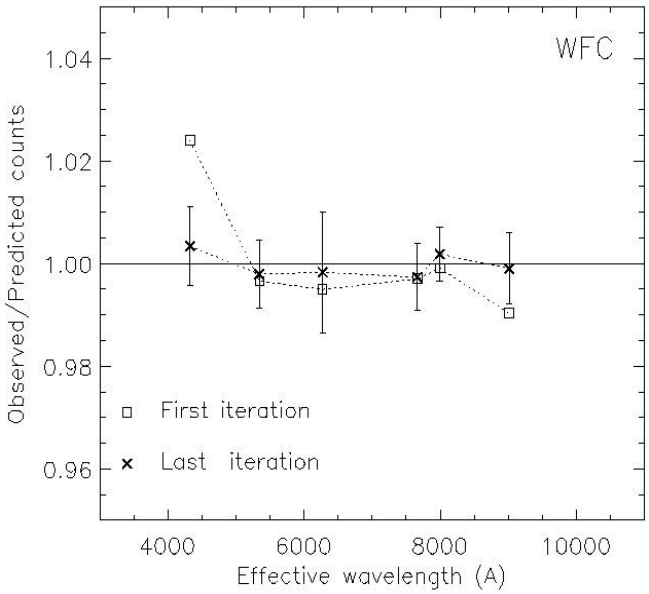

Figure 3: Comparison of observed/predicted ratios at the beginning(squares) and end (crosses) of the iterative process for the WFC. Error bars, from Table 1, are only shown for the final values.

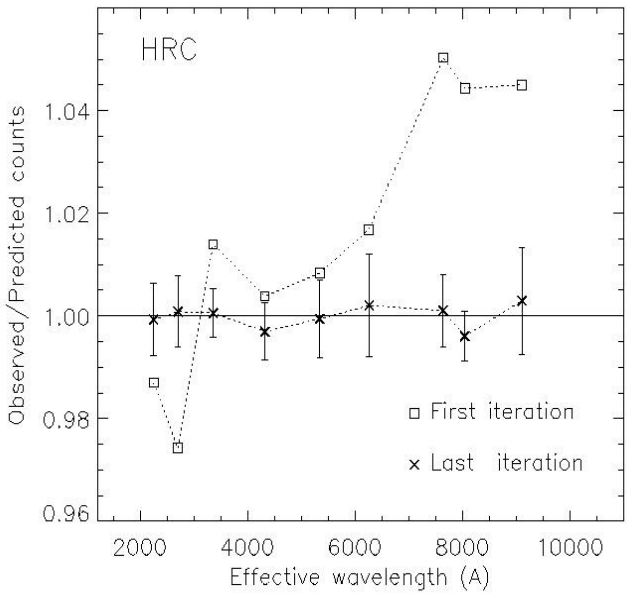

Figure 4: Comparison of observed/predicted ratios at the beginning (squares) and end (crosses) of the iterative process for the HRC. Error bars, from Table 1, are only shown for the final values.

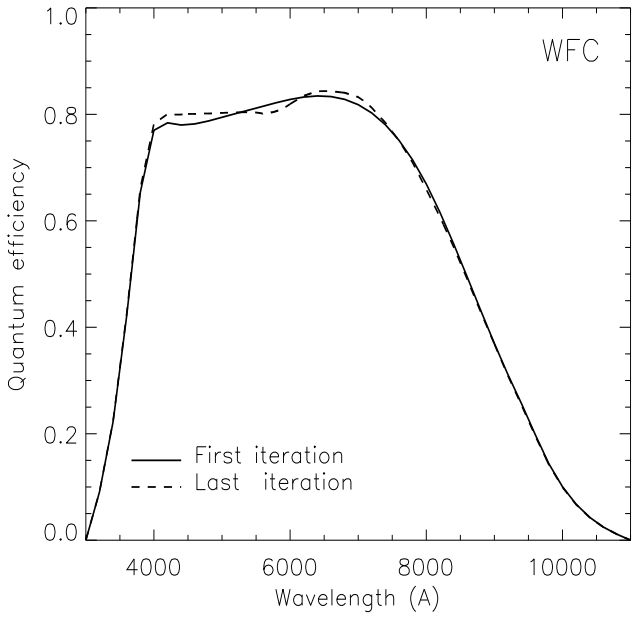

Figure 5: Comparison of initial (solid line) and final (dashed line) DQE for the WFC.

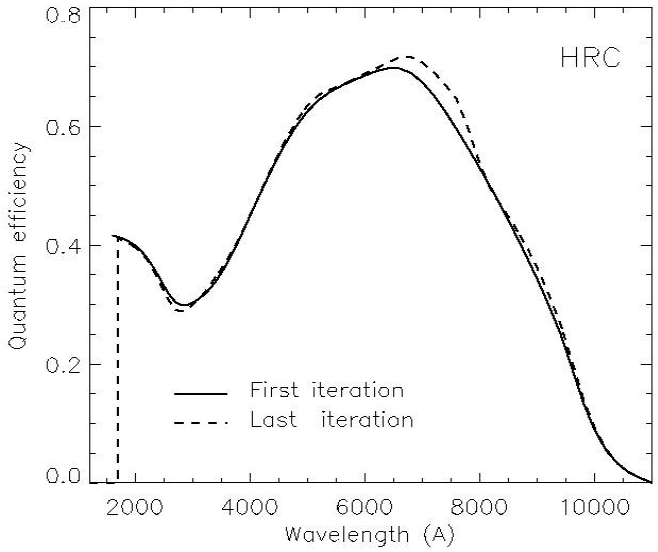

Figure 6: Comparison of initial (solid line) and final (dashed line) DQE for the HRC.

The rather smooth appearance of the DQE curves is the result of the regularizing effect of the smoothing applied in the second step of the iterative procedure indicated above. In particular, the data points corresponding to the ratio of observed and predicted count rates are first connected with a segmented line, which is then sampled at the wavelengths corresponding to the DQE data points. This line is then smoothed, by replacing the value corresponding to each wavelength with the average value over a range of 80 nm around it. The goal of this smoothing is to prevent measurement uncertainties from causing unphysical features in the DQE, such as bumps or spikes. For this reason, extending the number of iterations past the limits given above, at which convergence is reached, would not appreciably change the shape of the DQE.

With the DQE curves shown in Figures 5 and 6, Synphot is able to reproduce the observed count rates to within 0.5% in all broad band filters, with the exception of F606W and F475W (which were specifically excluded from the procedure, as indicated above). For these latter filters and for the narrow and medium band ones, Figures 7 and 8 show the ratio of observed and predicted counts when Synphot uses the DQE curves derived above, respectively for the WFC and HRC. As both figures show, the ratio of observed and predicted counts for narrow and medium band filters deviates from unity by as much as ~ 5%, but with values around 1% being more typical.

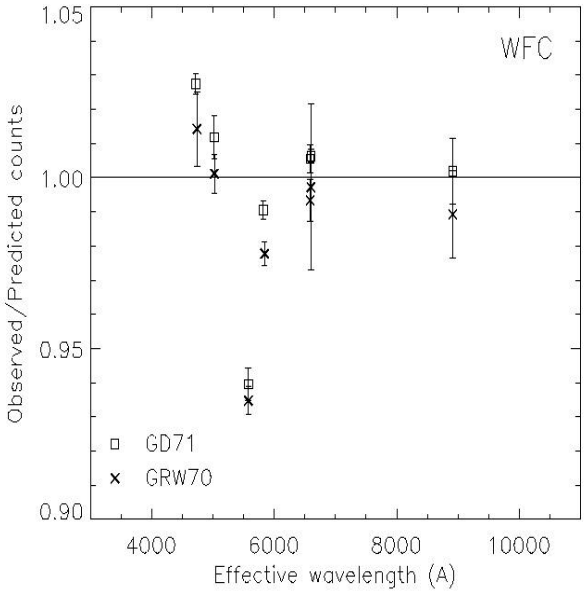

Figure 7: Observed/predicted count rates ratios for filters not part of the WFC iteration process before filter transmission correction. Squares refer to GD71, whilst crosses mark the GRW70 data.

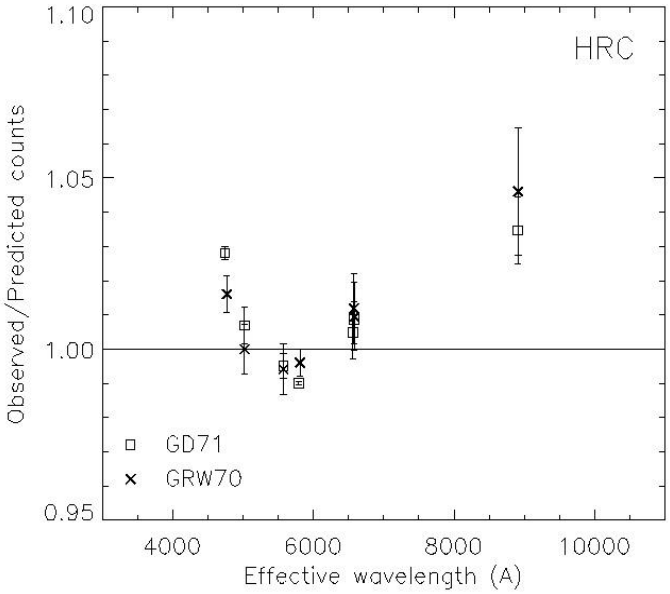

Figure 8: Observed/predicted count rates ratios for filters not part of the HRC iteration process before filter transmission correction. Squares refer to GD71, whilst crosses mark the GRW70 data.

The DQE has been determined over the whole wavelength range covered by the two CCD cameras on the basis of broad-band filter observations. Since it is reasonable to assume that over such a range the DQE should vary smoothly, one must conclude that the transmission curves of the narrow and medium band filters and of F606W and F475W must be updated to bring the ratio of observed and predicted counts as close as possible to unity. We stress here that, although ground measurements of the transmission curve can be affected by some uncertainty, the decision of updating the corresponding reference files in Synphot stems exclusively from our implicit assumption that the transmission curves of broad band filters are well characterised (with the notable exception of F606W and F475W, for the reasons explained above). In other words, the available data only allow us in general to characterise the combined photometric response of an observing mode, namely the combination of a detector and filter, rather than the individual components. However, as indicated in the Introduction, our adopted approach is satisfactory since our present goal is that of providing the photometric zero-point for the most common observing modes.

As regards the update of the filter transmission curves, we have elected to simply multiply them by a scale constant such that the ratio of observed and predicted counts is as close as possible to unity. Because the correction applied to a filter affects the ratio of observed and predicted counts for both cameras simultaneously, the filter being physically the same, the scale factor has been selected so that the ratio of observed and predicted counts is 1 on average for WFC and HRC for each of the filters affected. In general, no single value of the scale factor would bring the predicted WFC and HRC count rates in simultaneous agreement with the observations. So the scale factor has been determined to equally split between the WFC and HRC the departure of the ratio from unity. This is shown graphically in Figure 9, where the ratio of observed and predicted counts is shown separately for WFC (squares) and HRC (crosses) after the correction to the filter transmission curve. The scale factors for each filter are tabulated in Table 2.

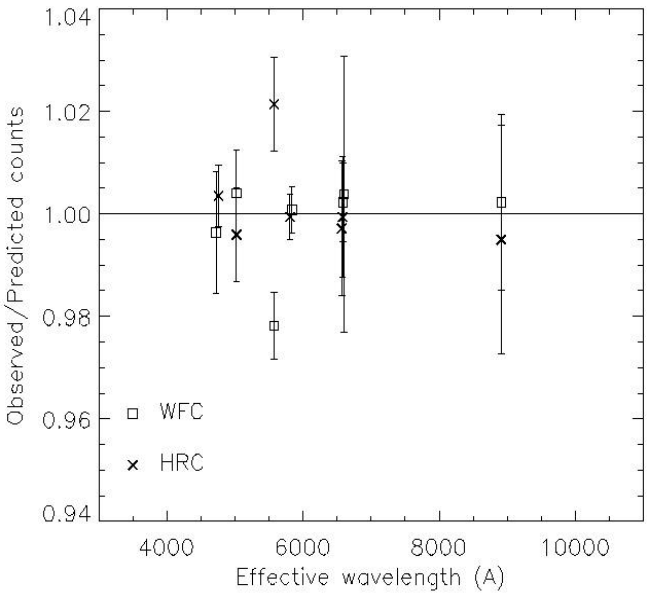

Figure 9: Observed/predicted count rates for narrow band filters for both WFC (squares) and HRC (crosses), after correction.

Table 2. Correction factors applied to the filter transmission curves previously used in Synphot to bring the predicted count rates in agreement with observations. Newly delivered filter transmission curves were multiplied by these coefficients.

FILTER	Correction Factor
F475W	1.0085
F502N	0.9920
F550M	0.9700
F606W	0.9810
F658N	0.9845
F660N	0.9865
F892N	0.9975

Although, as mentioned above, the WFC and HRC share the same filter complement (see the ACS instrument handbook for details; Pavlovsky et al. 2003), one must realise that different portions of the same filter illuminate the two CCDs, owing to the location of the ACS apertures in the HST focal plane. In particular, the light that reaches the HRC travels through a section of the filter much smaller than that affecting the WFC and it is, in principle, possible that the manufacturing of the filter (particularly of the narrow and medium band ones) might have left patches of uneven throughput across its face. Thus, by imposing the condition that the transmission curve of each filter be the same for both cameras, as is presently required by Synphot, we have made the implicit assumption that the filters are homogeneous across their face.

For broad band filters, since their flat field has been determined using observations of a calibration stellar field (47 Tuc) dithered across the FOV of the CCDs (Mack et al. 2002), any lack of uniformity of the bandpass average transmission across the filter face has been corrected by design. The flat field of narrow and medium band filters that the ACS pipeline currently uses is based on an interpolation of the flat field of the neighboring broad band filters. However, we do not presently know whether the throughput of narrow and medium band filters varies across the face of the filter and, if so, whether it varies in a way similar to that of broad band filters, as we have implicitly assumed. This assumption can be tested with available data, since repeated observations now exist of the same calibration stellar field (47 Tuc), at random orientation and in all narrow and medium band filters, with both cameras. This will permit a reliable measurement of the flat field in a similar way as it was done for broad band filters.

7. Conclusions: the Photometric Zero Points

With the information derived as explained in the sections above, we can derive the presently most reliable photometric zero points for the WFC and HRC in all three photometric systems used by Synphot, namely VEGAmag, STmag and ABmag. The zero points are given in Table 3.

Briefly, VEGAmag is Synphot's standard magnitude system, for which Vega by definition has magnitude 0 at all wavelengths. The VEGAmag magnitude of a star with flux F is -2.5 Log_{10} (F/F_{vega}) where F_{vega} is the calibrated spectrum of Vega in Synphot. STmag and ABmag are systems which define an equivalent flux density for a source, corresponding to the flux density of a source of predefined spectral shape that would produce the observed count rate, and convert this equivalent flux to a magnitude. The conversion is chosen so that the magnitude in V corresponds roughly to that in the Johnson system. In the STmag system, the flux density is expressed per unit wavelength, and the reference spectrum is flat in F_λ, whilst in the ABmag system the flux density is expressed per unit frequency and the reference spectrum is flat in F_ν. The definitions are:

$STmag = -2.5\ Log_{10}F_\lambda, -21.10$

$ABmag = -2.5\ Log_{10}F_\nu - 48.6$

where F_ν is expressed in erg cm^{-2} Hz^{-1} s^{-1} and F_λ, in erg cm^{-2} A^{-1} s^{-1}.

Another way to express these zero-points is to say that an object with F_λ, = 3.63 x 10^{-20} erg cm^{-2} Hz^{-1} s^{-1} will have magnitude ABmag=0 in every filter, and an object with F_λ, = 3.63 x 10^{-9} erg cm^{-2} A^{-1} s^{-1} will have magnitude STmag=0 in every filter. Finally, and more practically, one can think of the photometric zero points in Table 3 as the magnitude of an object that would generate a count-rate of 1 count/s in the specified observational configuration (i.e. combination of detector and filter).

The meaning of the columns in Table 3 is as follows:
+ FILTER: name of the bandpass;
+ PHOTPLAM: pivot wavelength of the filter plus detector configuration;
+ PHOTFLAM: inverse sensitivity of the configuration (erg cm^{-2} A^{-1} s^{-1}).
+ PHOTBW: rms bandwidth of filter plus detector configuration;
+ STmag, ABmag, VEGAmag: the zero points in the respective systems

The header keywords PHOTFLAM and PHOTPLAM relate to the STmag and ABmag zero-points through the formulae:

$STmag_{ZP} = -2.5\ Log_{10}$ (PHOTFLAM) - PHOTZPT

$= -2.5\ Log_{10}$ (PHOTFLAM) - 21.10

$ABmag_{ZP} = -2.5\ Log_{10}$ (PHOTFLAM) - 21.10 - 5 Log_{10} (PHOTPLAM) + 18.6921

As a final remark, we should like to note that the photometric zero points in the VEGAmag magnitude system given here are linked to the spectrum of Vega presently used by Synphot (Bohlin & Gilliland, 2004). An update of such a reference spectrum will require the zero points to be recalculated accordingly.

Table 3. Photometric zero points based on the newly derived DQE and filter transmission curves, for the WFC and HRC.

WFC

FILTER	PHOTPLAM	PHOTFLAM	PHOTBW	STmag	ABmag	VEGAmag
F435W	4317.398	3.141250E-19	293.47	25.157	25.673	25.779
F475W	4744.356	1.808802E-19	420.11	25.757	26.068	26.168
F502N	5022.475	5.326231E-18	41.89	22.084	22.271	22.352
F550M	5581.205	3.860100E-19	163.27	24.934	24.892	24.867
F555W	5359.547	1.955929E-19	360.02	25.672	25.718	25.724
F606W	5917.678	7.906457E-20	672.31	26.655	26.486	26.398
F625W	6310.454	1.195394E-19	415.46	26.206	25.898	25.731
F658N	6584.015	1.999181E-18	37.15	23.148	22.747	22.365
F660N	6599.374	5.347431E-18	35.53	22.081	21.676	21.389
F775W	7693.026	1.006545E-19	434.60	26.393	25.654	25.256
F814W	8059.761	7.072360E-20	654.64	26.776	25.937	25.501
F850LP	9054.768	1.507456E-19	539.43	25.954	24.862	24.326
F892N	8914.875	1.542548E-18	72.95	23.429	22.371	21.865

HRC

FILTER	PHOTPLAM	PHOTFLAM	PHOTBW	STmag	ABmag	VEGAmag
F220W	2255.426	8.113312E-18	187.28	21.627	23.553	21.871
F250W	2715.875	4.781345E-18	239.40	22.201	23.724	22.288
F330W	3362.675	2.236720E-18	173.82	23.026	24.085	22.904
F344N	3432.847	2.139635E-17	42.62	20.574	21.588	20.439
F435W	4310.986	5.368556E-19	309.68	24.575	25.095	25.185
F475W	4775.74	2.937020E-19	418.81	25.230	25.527	25.623
F502N	5021.072	8.034045E-18	83.01	21.638	21.826	21.906
F550M	5579.729	5.985392E-19	168.05	24.457	24.416	24.392
F555W	5355.946	3.020066E-19	357.19	25.200	25.248	25.255

F606W	5887.935	1.278104E-19	664.88	26.134	25.976	25.893
F625W	6295.498	1.973001E-19	415.31	25.662	25.359	25.195
F658N	6581.98	3.357119E-18	162.69	22.585	22.185	21.803
F660N	6582.439	8.976461E-18	468.30	21.516	21.116	20.827
F775W	7665.083	1.949664E-19	432.03	25.675	24.945	24.551
F814W	8115.338	1.269102E-19	703.45	26.141	25.287	24.849
F850LP	9145.236	2.286987E-19	538.95	25.502	24.388	23.850
F892N	8913.882	2.447032E-18	270.92	22.928	21.870	21.366

References

Bohlin, R. 1995, in Calibrating Hubble Space Telescope, Eds A. Koratkar, C. Leitherer (Baltimore: STScI), 49

Bohlin, R. & Gilliland, R. 2004, AJ in press.

Mack, J., Bohlin, R., Gilliland, R., van der Marel, R., De Marchi, G. 2002, in 2002 HST Calibration Workshop, Eds. S. Arribas, A. Koekemoer, B. Whitmore (Baltimore: STScI), 23

Gilliland, R., Riess, A. 2002, in 2002 HST Calibration Workshop, Eds. S. Arribas, A. Koekemoer, B. Whitmore (Baltimore: STScI), 61

Oke, J.B. 1990, AJ, 99, 1621.

Pavlovsky et al. 2003 ACS Instrument Handbook, STScI.

Sirianni, M., De Marchi, G., Gilliland, R., Bohlin, R., Pavlovsky, C., Mack, J. 2002a, in 2002 HST Calibration Workshop, Eds. S. Arribas, A. Koekemoer, B. Whitmore (Baltimore: STScI), 31

Sirianni, M., Martel, A., Jee, M., Van Orsow, D., Sparks, W. 2002b, in 2002 HST Calibration Workshop, Eds. S. Arribas, A. Koekemoer, B. Whitmore (Baltimore: STScI), 82

Sirianni, M., et al. 2004. PASP in preparation

APPENDIX

Table 4. List of ACS datasets that were used in this investigation. The columns are the target name, the rootname of the data file, the date of the observation, the exposure time, the filter name, the camera and the flat field used.

Target	Dataset	Date	Time	EXP time	FILTER	Camera	Flat Field (.fits)
GD7	j8c107010	2002-04-12	09:14:54 am	10	F475W	HRC	mag13035j_pfl
GD71	j8c107020	2002-04-12	09:17:10 am	360	F502N	HRC	m9b1221oj_pfl
GD71	j8c107030	2002-04-12	09:25:29 am	40	F550M	HRC	m9b1221pj_pfl
GD71	j8c107040	2002-04-12	09:28:16 am	18	F555W	HRC	m9b1221qj_pfl
GD71	j8c107050	2002-04-12	09:30:51 am	10	F606W	HRC	m9b1221rj_pfl
GD71	j8c107060	2002-04-12	09:33:20 am	20	F625W	HRC	mag13036j_pfl
GD71	j8c107070	2002-04-12	09:35:52 am	480	F658N	HRC	m9b1221tj_pfl
GD71	j8c107080	2002-04-12	09:45:57 am	50	F775W	HRC	m9b12221j_pfl
GD71	j8c107090	2002-04-12	09:48:55 am	100	F850LP	HRC	mag13037j_pfl
GD71	j8c1070a0	2002-04-12	10:39:58 am	600	F892N	HRC	m9b12224j_pfl
GD71	j8c1070b0	2002-04-12	10:52:17 am	12	F435W	HRC	mag13034j_pfl
GD71	j8c1070c0	2002-04-12	10:54:34 am	1200	F660N	HRC	m9b12220j_pfl
GD71	j8c1070d0	2002-04-12	11:16:28 am	40	F814W	HRC	m9b12222j_pfl
GD71	j8c1070e0	2002-04-12	11:19:27 am	12	F220W	HRC	n4t15308j_pfl
GD71	j8c1070f0	2002-04-12	11:21:43 am	12	F250W	HRC	n4t1530aj_pfl
GD71	j8c1070g0	2002-04-12	12:16:03 pm	160	F344N	HRC	n4t1530cj_pfl
GD71	j8c1070u0	2002-04-12	02:23:54 pm	14	F330W	HRC	n4t1530bj_pfl
GRW+70	j8eg07010	2002-07-13	03:55:57 am	10	F475W	HRC	mag13035j_pfl
GRW+70	j8eg07020	2002-07-13	03:58:13 am	300	F502N	HRC	m9b1221oj_pfl
GRW+70	j8eg07030	2002-07-13	04:05:32 am	40	F550M	HRC	m9b1221pj_pfl
GRW+70	j8eg07040	2002-07-13	04:08:19 am	18	F555W	HRC	m9b1221qj_pfl
GRW+70	j8eg07050	2002-07-13	04:10:54 am	10	F606W	HRC	m9b1221rj_pfl
GRW+70	j8eg07060	2002-07-13	04:13:23 am	18	F625W	HRC	mag13036j_pfl
GRW+70	j8eg07070	2002-07-13	04:15:53 am	430	F658N	HRC	m9b1221tj_pfl
GRW+70	j8eg07080	2002-07-13	04:25:08 am	40	F775W	HRC	m9b12221j_pfl
GRW+70	j8eg07090	2002-07-13	04:27:56 am	110	F850LP	HRC	mag13037j_pfl
GRW+70	j8eg070a0	2002-07-13	04:31:52 am	600	F892N	HRC	m9b12224j_pfl
GRW+70	j8eg070b0	2002-07-13	05:26:42 am	12	F435W	HRC	mag13034j_pfl

GRW+70	j8eg070c0	2002-07-13	05:28:59 am	1200	F660N	HRC	m9b12220j_pfl
GRW+70	j8eg070d0	2002-07-13	05:50:53 am	35	F814W	HRC	m9b12222j_pfl
GRW+70	j8eg070e0	2002-07-13	05:53:48 am	12	F220W	HRC	m9b1222ej_pfl
GRW+70	j8eg070f0	2002-07-13	05:56:04 am	16	F250W	HRC	m9b1222aj_pfl
GRW+70	j8eg070g0	2002-07-13	05:58:20 am	17	F330W	HRC	m9b12225j_pfl
GRW+70	j8eg070h0	2002-07-13	06:00:43 am	190	F344N	HRC	m9b12226j_pfl
GRW+70	j8eg08010	2002-08-10	08:41:28 am	10	F475W	HRC	mag13035j_pfl
GRW+70	j8eg08020	2002-08-10	08:43:44 am	300	F502N	HRC	m9b1221oj_pfl
GRW+70	j8eg08030	2002-08-10	08:51:03 am	40	F550M	HRC	m9b1221pj_pfl
GRW+70	j8eg08040	2002-08-10	08:53:50 am	18	F555W	HRC	m9b1221qj_pfl
GRW+70	j8eg08050	2002-08-10	08:56:25 am	10	F606W	HRC	m9b1221rj_pfl
GRW+70	j8eg08060	2002-08-10	08:58:54 am	18	F625W	HRC	mag13036j_pfl
GRW+70	j8eg08070	2002-08-10	09:01:24 am	430	F658N	HRC	m9b1221tj_pfl
GRW+70	j8eg08080	2002-08-10	09:10:39 am	40	F775W	HRC	m9b12221j_pfl
GRW+70	j8eg08090	2002-08-10	09:13:27 am	110	F850LP	HRC	mag13037j_pfl
GRW+70	j8eg080a0	2002-08-10	09:17:23 am	600	F892N	HRC	m9b12224j_pfl
GRW+70	j8eg080b0	2002-08-10	10:12:17 am	12	F435W	HRC	mag13034j_pfl
GRW+70	j8eg080c0	2002-08-10	10:14:34 am	1200	F660N	HRC	m9b12220j_pfl
GRW+70	j8eg080d0	2002-08-10	10:36:28 am	35	F814W	HRC	m9b12222j_pfl
GRW+70	j8eg080e0	2002-08-10	10:39:23 am	12	F220W	HRC	m9b1222ej_pfl
GRW+70	j8eg080f0	2002-08-10	10:41:39 am	16	F250W	HRC	m9b1222aj_pfl
GRW+70	j8eg080g0	2002-08-10	10:43:55 am	17	F330W	HRC	m9b12225j_pfl
GRW+70	j8eg09010	2002-09-14	10:03:08 pm	10	F475W	HRC	mag13035j_pfl
GRW+70	j8eg09020	2002-09-14	10:05:24 pm	300	F502N	HRC	m9b1221oj_pfl
GRW+70	j8eg09030	2002-09-14	10:12:42 pm	40	F550M	HRC	m9b1221pj_pfl
GRW+70	j8eg09040	2002-09-14	10:15:29 pm	18	F555W	HRC	m9b1221qj_pfl
GRW+70	j8eg09050	2002-09-14	10:18:05 pm	10	F606W	HRC	m9b1221rj_pfl
GRW+70	j8eg09060	2002-09-14	10:20:33 pm	18	F625W	HRC	mag13036j_pfl
GRW+70	j8eg09070	2002-09-14	10:23:04 pm	430	F658N	HRC	m9b1221tj_pfl
GRW+70	j8eg09080	2002-09-14	10:32:18 pm	40	F775W	HRC	m9b12221j_pfl
GRW+70	j8eg09090	2002-09-14	10:35:06 pm	110	F850LP	HRC	mag13037j_pfl
GRW+70	j8eg090a0	2002-09-14	10:39:02 pm	600	F892N	HRC	m9b12224j_pfl
GRW+70	j8eg090b0	2002-09-14	11:25:13 pm	12	F435W	HRC	mag13034j_pfl
GRW+70	j8eg090c0	2002-09-14	11:27:29 pm	1200	F660N	HRC	m9b12220j_pfl

GRW+70	j8eg090d0	2002-09-14	11:49:24 pm	35	F814W	HRC	m9b12222j_pfl
GRW+70	j8eg090e0	2002-09-14	11:52:18 pm	12	F220W	HRC	m9b1222ej_pfl
GRW+70	j8eg090f0	2002-09-14	11:54:34 pm	16	F250W	HRC	m9b1222aj_pfl
GRW+70	j8eg090g0	2002-09-14	11:56:50 pm	17	F330W	HRC	m9b12225j_pfl
GRW+70	j8eg090h0	2002-09-14	11:59:13 pm	190	F344N	HRC	m9b12226j_pfl
GRW+70	j8hv03010	2002-12-13	06:27:04 pm	60	F220W	HRC	m9b1222ej_pfl
GRW+70	j8hv03020	2002-12-13	06:30:08 pm	60	F250W	HRC	m9b1222aj_pfl
GRW+70	j8hv03030	2002-12-13	06:33:08 pm	50	F330W	HRC	m9b12225j_pfl
GRW+70	j8hv03040	2002-12-13	06:36:45 pm	60	F220W	HRC	m9b1222ej_pfl
GRW+70	j8hv03050	2002-12-13	06:39:49 pm	60	F250W	HRC	m9b1222aj_pfl
GRW+70	j8hv03060	2002-12-13	06:42:49 pm	50	F330W	HRC	m9b12225j_pfl
GRW+70	j8hv03070	2002-12-13	06:50:45 pm	60	F220W	HRC	m9b1222ej_pfl
GRW+70	j8hv03080	2002-12-13	06:53:49 pm	60	F250W	HRC	m9b1222aj_pfl
GRW+70	j8hv03090	2002-12-13	06:56:49 pm	50	F330W	HRC	m9b12225j_pfl
GRW+70	j8hv04010	2003-01-12	12:24:03 am	60	F220W	HRC	m9b1222ej_pfl
GRW+70	j8hv04020	2003-01-12	12:27:07 am	60	F250W	HRC	m9b1222aj_pfl
GRW+70	j8hv04030	2003-01-12	12:30:07 am	50	F330W	HRC	m9b12225j_pfl
GRW+70	j8hv04040	2003-01-12	12:33:24 am	60	F220W	HRC	m9b1222ej_pfl
GRW+70	j8hv04050	2003-01-12	12:36:28 am	60	F250W	HRC	m9b1222aj_pfl
GRW+70	j8hv04060	2003-01-12	12:39:28 am	50	F330W	HRC	m9b12225j_pfl
GRW+70	j8hv04070	2003-01-12	12:47:04 am	60	F220W	HRC	m9b1222ej_pfl
GRW+70	j8hv04080	2003-01-12	12:50:08 am	60	F250W	HRC	m9b1222aj_pfl
GRW+70	j8hv04090	2003-01-12	12:53:08 am	50	F330W	HRC	m9b12225j_pfl
GRW+70	j8jq02010	2003-02-26	10:04:29 am	10	F475W	HRC	mag13035j_pfl
GRW+70	j8jq02020	2003-02-26	10:06:45 am	300	F502N	HRC	m9b1221oj_pfl
GRW+70	j8jq02030	2003-02-26	10:14:04 am	40	F550M	HRC	m9b1221pj_pfl
GRW+70	j8jq02040	2003-02-26	10:16:51 am	18	F555W	HRC	m9b1221qj_pfl
GRW+70	j8jq02050	2003-02-26	10:19:26 am	10	F606W	HRC	m9b1221rj_pfl
GRW+70	j8jq02060	2003-02-26	10:21:55 am	18	F625W	HRC	mag13036j_pfl
GRW+70	j8jq02070	2003-02-26	10:24:25 am	430	F658N	HRC	m9b1221tj_pfl
GRW+70	j8jq02080	2003-02-26	10:33:40 am	40	F775W	HRC	m9b12221j_pfl
GRW+70	j8jq02090	2003-02-26	10:36:28 am	110	F850LP	HRC	mag13037j_pfl
GRW+70	j8jq020a0	2003-02-26	10:40:24 am	600	F892N	HRC	m9b12224j_pfl
GRW+70	j8jq020b0	2003-02-26	11:34:05 am	12	F435W	HRC	mag13034j_pfl

GRW+70	j8jq020c0	2003-02-26	11:36:22 am	1200	F660N	HRC	m9b12220j_pfl
GRW+70	j8jq020d0	2003-02-26	11:58:16 am	35	F814W	HRC	m9b12222j_pfl
GRW+70	j8jq020e0	2003-02-26	12:01:11 pm	12	F220W	HRC	m9b1222ej_pfl
GRW+70	j8jq020f0	2003-02-26	12:03:27 pm	16	F250W	HRC	m9b1222aj_pfl
GRW+70	j8jq020g0	2003-02-26	12:05:44 pm	190	F344N	HRC	m9b12226j_pfl
GRW+70	j8jq020q0	2003-02-26	01:36:07 pm	17	F330W	HRC	m9b12225j_pfl
GD71	j8c103010	2002-04-24	11:26:04 am	3	F475W	WFC	m820832fj_pfl
GD71	j8c103020	2002-04-24	11:28:49 am	90	F502N	WFC	m820832gj_pfl
GD71	j8c103030	2002-04-24	11:33:10 am	10	F550M	WFC	m820832hj_pfl
GD71	j8c103040	2002-04-24	11:36:01 am	4.6	F555W	WFC	m820832ij_pfl
GD71	j8c103050	2002-04-24	11:39:00 am	2.6	F606W	WFC	m820832jj_pfl
GD71	j8c103060	2002-04-24	11:41:55 am	5	F625W	WFC	m820832kj_pfl
GD71	j8c103070	2002-04-24	11:44:50 am	120	F658N	WFC	m820832lj_pfl
GD71	j8c103080	2002-04-24	11:49:36 am	9	F775W	WFC	m820832nj_pfl
GD71	j8c103090	2002-04-24	11:52:28 am	24	F850LP	WFC	m820832pj_pfl
GD71	j8c1030a0	2002-04-24	11:56:41 am	220	F892N	WFC	m820832qj_pfl
GD71	j8c1030g0	2002-04-24	01:11:09 pm	4	F435W	WFC	m820832ej_pfl
GD71	j8c1030h0	2002-04-24	01:13:55 pm	300	F660N	WFC	m820832mj_pfl
GD71	j8c1030i0	2002-04-24	01:21:29 pm	8	F814W	WFC	m820832oj_pfl
GD71	j8c1030j0	2002-04-24	01:25:15 pm	8	F814W	WFC	m820832oj_pfl
GD71	j8c104010	2002-04-16	02:52:04 am	3	F475W	WFC	m820832fj_pfl
GD71	j8c104020	2002-04-16	02:54:49 am	90	F502N	WFC	m820832gj_pfl
GD71	j8c104030	2002-04-16	02:59:10 am	10	F550M	WFC	m820832hj_pfl
GD71	j8c104040	2002-04-16	03:02:01 am	4.6	F555W	WFC	m820832ij_pfl
GD71	j8c104050	2002-04-16	03:05:00 am	2.6	F606W	WFC	m820832jj_pfl
GD71	j8c104060	2002-04-16	03:07:55 am	5	F625W	WFC	m820832kj_pfl
GD71	j8c104070	2002-04-16	03:10:50 am	120	F658N	WFC	m820832lj_pfl
GD71	j8c104080	2002-04-16	03:15:36 am	9	F775W	WFC	m820832nj_pfl
GD71	j8c104090	2002-04-16	03:18:28 am	24	F850LP	WFC	m820832pj_pfl
GD71	j8c1040a0	2002-04-16	03:22:10 am	4	F435W	WFC	m820832ej_pfl
GD71	j8c1040b0	2002-04-16	03:24:56 am	300	F660N	WFC	m820832mj_pfl
GRW+70	j8eg04010	2002-07-11	04:08:46 am	2	F475W	WFC	m820832fj_pfl
GRW+70	j8eg04020	2002-07-11	04:11:29 am	52	F502N	WFC	m820832gj_pfl
GRW+70	j8eg04030	2002-07-11	04:15:11 am	2.8	F555W	WFC	m820832ij_pfl

GRW+70	j8eg04040	2002-07-11	04:18:08 am	1.6	F606W	WFC	m820832jj_pfl
GRW+70	j8eg04050	2002-07-11	04:21:01 am	3.2	F625W	WFC	m820832kj_pfl
GRW+70	j8eg04060	2002-07-11	04:23:54 am	72	F658N	WFC	m820832lj_pfl
GRW+70	j8eg04070	2002-07-11	04:27:52 am	5	F775W	WFC	m820832nj_pfl
GRW+70	j8eg04080	2002-07-11	04:30:40 am	16	F850LP	WFC	m820832pj_pfl
GRW+70	j8eg04090	2002-07-11	05:18:19 am	140	F892N	WFC	m820832qj_pfl
GRW+70	j8eg040a0	2002-07-11	05:29:13 am	2.6	F435W	WFC	m820832ej_pfl
GRW+70	j8eg040b0	2002-07-11	05:31:55 am	4.4	F814W	WFC	m820832oj_pfl
GRW+70	j8eg040c0	2002-07-11	05:36:18 am	2	F475W	WFC	m820832fj_pfl
GRW+70	j8eg040d0	2002-07-11	06:54:24 am	52	F502N	WFC	m820832gj_pfl
GRW+70	j8eg040e0	2002-07-11	06:58:06 am	2.8	F555W	WFC	m820832ij_pfl
GRW+70	j8eg040f0	2002-07-11	07:01:03 am	1.6	F606W	WFC	m820832jj_pfl
GRW+70	j8eg040g0	2002-07-11	07:03:56 am	3.2	F625W	WFC	m820832kj_pfl
GRW+70	j8eg040h0	2002-07-11	07:06:49 am	72	F658N	WFC	m820832lj_pfl
GRW+70	j8eg040i0	2002-07-11	07:10:47 am	5	F775W	WFC	m820832nj_pfl
GRW+70	j8eg040j0	2002-07-11	07:13:35 am	16	F850LP	WFC	m820832pj_pfl
GRW+70	j8eg040k0	2002-07-11	07:17:09 am	2.6	F435W	WFC	m820832ej_pfl
GRW+70	j8eg040l0	2002-07-11	07:19:51 am	4.4	F814W	WFC	m820832oj_pfl
GRW+70	j8eg05010	2002-08-18	12:45:02 am	2	F475W	WFC	m820832fj_pfl
GRW+70	j8eg05020	2002-08-18	12:47:45 am	52	F502N	WFC	m820832gj_pfl
GRW+70	j8eg05030	2002-08-18	12:51:27 am	2.8	F555W	WFC	m820832ij_pfl
GRW+70	j8eg05040	2002-08-18	12:54:24 am	1.6	F606W	WFC	m820832jj_pfl
GRW+70	j8eg05050	2002-08-18	12:57:17 am	3.2	F625W	WFC	m820832kj_pfl
GRW+70	j8eg05060	2002-08-18	01:00:10 am	72	F658N	WFC	m820832lj_pfl
GRW+70	j8eg05070	2002-08-18	01:04:08 am	5	F775W	WFC	m820832nj_pfl
GRW+70	j8eg05080	2002-08-18	01:06:56 am	16	F850LP	WFC	m820832pj_pfl
GRW+70	j8eg05090	2002-08-18	01:11:01 am	140	F892N	WFC	m820832qj_pfl
GRW+70	j8eg050a0	2002-08-18	01:21:55 am	2.6	F435W	WFC	m820832ej_pfl
GRW+70	j8eg050b0	2002-08-18	01:24:37 am	4.4	F814W	WFC	m820832oj_pfl
GRW+70	j8eg050c0	2002-08-18	01:29:00 am	2	F475W	WFC	m820832fj_pfl
GRW+70	j8eg050d0	2002-08-18	02:16:17 am	52	F502N	WFC	m820832gj_pfl
GRW+70	j8eg050e0	2002-08-18	02:19:59 am	2.8	F555W	WFC	m820832ij_pfl
GRW+70	j8eg050f0	2002-08-18	02:22:56 am	1.6	F606W	WFC	m820832jj_pfl
GRW+70	j8eg050g0	2002-08-18	02:25:49 am	3.2	F625W	WFC	m820832kj_pfl

GRW+70	j8eg050h0	2002-08-18	02:28:42 am	72	F658N	WFC	m820832lj_pfl
GRW+70	j8eg050i0	2002-08-18	02:32:40 am	5	F775W	WFC	m820832nj_pfl
GRW+70	j8eg050j0	2002-08-18	02:35:28 am	16	F850LP	WFC	m820832pj_pfl
GRW+70	j8eg050k0	2002-08-18	02:39:02 am	2.6	F435W	WFC	m820832ej_pfl
GRW+70	j8eg050l0	2002-08-18	02:41:44 am	4.4	F814W	WFC	m820832oj_pfl
GRW+70	j8eg06010	2002-09-13	06:45:52 pm	2	F475W	WFC	m820832fj_pfl
GRW+70	j8eg06020	2002-09-13	06:48:35 pm	52	F502N	WFC	m820832gj_pfl
GRW+70	j8eg06030	2002-09-13	06:52:16 pm	2.8	F555W	WFC	m820832ij_pfl
GRW+70	j8eg06040	2002-09-13	06:55:13 pm	1.6	F606W	WFC	m820832jj_pfl
GRW+70	j8eg06050	2002-09-13	06:58:07 pm	3.2	F625W	WFC	m820832kj_pfl
GRW+70	j8eg06060	2002-09-13	07:01:00 pm	72	F658N	WFC	m820832lj_pfl
GRW+70	j8eg06070	2002-09-13	07:04:57 pm	5	F775W	WFC	m820832nj_pfl
GRW+70	j8eg06080	2002-09-13	07:07:45 pm	16	F850LP	WFC	m820832pj_pfl
GRW+70	j8eg06090	2002-09-13	07:11:51 pm	140	F892N	WFC	m820832qj_pfl
GRW+70	j8eg060a0	2002-09-13	07:22:44 pm	2.6	F435W	WFC	m820832ej_pfl
GRW+70	j8eg060b0	2002-09-13	07:25:27 pm	4.4	F814W	WFC	m820832oj_pfl
GRW+70	j8eg060c0	2002-09-13	08:09:59 pm	2	F475W	WFC	m820832fj_pfl
GRW+70	j8eg060d0	2002-09-13	08:40:01 pm	52	F502N	WFC	m820832gj_pfl
GRW+70	j8eg060e0	2002-09-13	08:43:44 pm	2.8	F555W	WFC	m820832ij_pfl
GRW+70	j8eg060f0	2002-09-13	08:46:40 pm	1.6	F606W	WFC	m820832jj_pfl
GRW+70	j8eg060g0	2002-09-13	08:49:33 pm	3.2	F625W	WFC	m820832kj_pfl
GRW+70	j8eg060h0	2002-09-13	08:52:27 pm	72	F658N	WFC	m820832lj_pfl
GRW+70	j8eg060i0	2002-09-13	08:56:24 pm	5	F775W	WFC	m820832nj_pfl
GRW+70	j8eg060j0	2002-09-13	08:59:12 pm	16	F850LP	WFC	m820832pj_pfl
GRW+70	j8eg060k0	2002-09-13	09:02:47 pm	2.6	F435W	WFC	m820832ej_pfl
GRW+70	j8eg060l0	2002-09-13	09:05:28 pm	4.4	F814W	WFC	m820832oj_pfl
GRW+70	j8jq03060	2003-01-16	03:30:16 am	2	F475W	WFC	m820832fj_pfl
GRW+70	j8jq03070	2003-01-16	03:32:59 am	52	F502N	WFC	m820832gj_pfl
GRW+70	j8jq03080	2003-01-16	03:36:42 am	5.2	F550M	WFC	m820832hj_pfl
GRW+70	j8jq03090	2003-01-16	03:39:29 am	2.8	F555W	WFC	m820832ij_pfl
GRW+70	j8jq030a0	2003-01-16	03:42:26 am	1.6	F606W	WFC	m820832jj_pfl
GRW+70	j8jq030b0	2003-01-16	03:45:19 am	3.2	F625W	WFC	m820832kj_pfl
GRW+70	j8jq030c0	2003-01-16	03:48:12 am	72	F658N	WFC	m820832lj_pfl
GRW+70	j8jq030d0	2003-01-16	03:52:20 am	200	F660N	WFC	m820832mj_pfl

GRW+70	j8jq030e0	2003-01-16	03:58:36 am	5	F775W	WFC	m820832nj_pfl
GRW+70	j8jq04010	2003-01-15	02:11:21 am	16	F850LP	WFC	m820832pj_pfl
GRW+70	j8jq04020	2003-01-15	02:14:55 am	2.6	F435W	WFC	m820832ej_pfl
GRW+70	j8jq04030	2003-01-15	02:17:37 am	4.4	F814W	WFC	m820832oj_pfl
GRW+70	j8jq04040	2003-01-15	02:21:45 am	140	F892N	WFC	m820832qj_pfl
GRW+70	j8jq040a0	2003-01-15	02:48:31 am	2	F475W	WFC	m820832fj_pfl
GRW+70	j8jq040b0	2003-01-15	02:51:14 am	52	F502N	WFC	m820832gj_pfl
GRW+70	j8jq040c0	2003-01-15	02:54:56 am	2.8	F555W	WFC	m820832ij_pfl
GRW+70	j8jq040d0	2003-01-15	02:57:53 am	1.6	F606W	WFC	m820832jj_pfl
GRW+70	j8jq05010	2003-01-15	04:17:00 am	3.2	F625W	WFC	m820832kj_pfl
GRW+70	j8jq05020	2003-01-15	04:19:53 am	72	F658N	WFC	m820832lj_pfl
GRW+70	j8jq05030	2003-01-15	04:24:01 am	100	F660N	WFC	m820832mj_pfl
GRW+70	j8jq05040	2003-01-15	04:28:37 am	5	F775W	WFC	m820832nj_pfl
GRW+70	j8jq05050	2003-01-15	04:31:25 am	16	F850LP	WFC	m820832pj_pfl
GRW+70	j8jq05060	2003-01-15	04:34:59 am	2.6	F435W	WFC	m820832ej_pfl
GRW+70	j8jq05070	2003-01-15	04:37:41 am	4.4	F814W	WFC	m820832oj_pfl